







Profiles of oral microbiome associated with nasogastric tube feeding

Ding-Han Wang ^a, Fa-Tzu Tsai ^a, Hsi-Feng Tu ^{a,b}, Cheng-Chieh Yang ^{a,c}, Ming-Lun Hsu ^a, Lin-Jack Huang^b, Chiu-Tzu Lin^b, Wun-Eng Hsu^d and Yu-Cheng Lin ^a

^aDepartment of Dentistry, National Yang Ming Chiao Tung University, Taipei, Taiwan; ^bDepartment of Dentistry, National Yang Ming Chiao Tung University Hospital, Yilan County, Taiwan; ^cDepartment of Stomatology, Oral & Maxillofacial Surgery, Taipei Veterans General Hospital, Taipei, Taiwan; ^dDepartment of Dentistry, Far Eastern Memorial Hospital, New Taipei, Taiwan

ABSTRACT

Background: Dysbiosis of oral microbiome causes chronic diseases including dental caries and periodontitis, which frequently affect older patient populations. Severely disabled individuals with impaired swallowing functions may require nutritional supply via nasogastric (NG) tubes, further impacting their oral condition and possibly microbial composition. However, little is known about the effect of NG tube on oral microbes and its potential ramification.

Methods: By using 16S rRNA amplicon sequencing, we characterized the tongue microbiome of 27 patients fed with NG tubes and 26 others fed orally.

Results: The microbial compositions of NG-tube and oral-feeding patients were substantially different, with more Gram-negative aerobes enriched in the presence of NG tube. Specifically, NG-tube patients presented more opportunistic pathogens like *Pseudomonas* and *Corynebacterium* associated with pneumonia and lower levels of commensal *Streptococcus* and *Veillonella*. Co-occurrence analysis further showed an inverse relationship between commensal and pathogenic species.

Conclusion: We present a systematic, high-throughput profiling of oral microbiome with regard to long-term NG tube feeding among the older patient population.

ARTICLE HISTORY

Received 27 September 2022
Revised 28 December 2022
Accepted 4 April 2023

KEYWORDS

Oral microbiome;
nasogastric tube; 16S rRNA;
amplicon sequence variant;
aspiration pneumonia

Introduction


The human oral cavity hosts hundreds of microbial species which play a crucial role in both oral and general health [1–3]. Imbalanced oral microbiome, i.e. dysbiosis, is the primary causal factor of various oral and systemic diseases including dental caries, periodontitis [2] and infectious endocarditis [4]. In addition, oral dysbiosis was shown to be associated with oral cancer, colorectal cancer, pancreatic cancer, rheumatoid arthritis, Alzheimer's disease and diabetes, yet definitive evidence for causal relationships is still lacking [2,5]. In the past, the emergence of specific bacterial species was often viewed as the singular cause of chronic oral diseases; however, recent advancements in high-throughput sequencing technology led to the notion that dysbiosis is a polymicrobial condition resulted from the complex interplay between the host and microbial community [6,7]. Oral dysbiosis often results in chronic illnesses which are particularly common in older patient populations [8].

Older and disabled patients are more often to receive long-term care, which is a challenging situation for both caregivers and patients. One of the main

factors affecting these patients' life quality is how nutrition is fed through the enteral route. Besides the normal oral intake, patients with cognitive impairment or swallowing difficulty require tube-feeding methods such as percutaneous endoscopic gastrostomy tube and nasogastric (NG) tube [9], the latter being the most common. During NG tube-feeding, patients' normal oral function (e.g. chewing and swallowing) is significantly compromised. These patients were often cognitively impaired and thus may suffer from poor oral hygiene care [10], negatively impacting their oral microbial community and general health conditions. Although NG-tube feeding could be beneficial for the patients in the short term to deal with malnutrition [11], patients with prolonged tube feeding often suffered from dysphagia [12], malnutrition [13] and aspiration pneumonia [14].

Aspiration pneumonia, an acute condition caused by inhalation of oropharyngeal pathogens, poses major mortality risks to patients with NG tube as these patients often have impaired swallowing and cough reflux [15,16]. The presence of NG tube has been suggested to be associated with aspiration

CONTACT Yu-Cheng Lin  ylin@nycu.edu.tw 

 Supplemental data for this article can be accessed online at <https://doi.org/10.1080/20002297.2023.2200898>.

© 2023 The Author(s). Published by Informa UK Limited, trading as Taylor & Francis Group.

This is an Open Access article distributed under the terms of the Creative Commons Attribution-NonCommercial License (<http://creativecommons.org/licenses/by-nc/4.0/>), which permits unrestricted non-commercial use, distribution, and reproduction in any medium, provided the original work is properly cited. The terms on which this article has been published allow the posting of the Accepted Manuscript in a repository by the author(s) or with their consent.

pneumonia, though the pathogen could originate from either oropharyngeal or gastric routes [17]. Aspiration pneumonia is most commonly treated with empiric antimicrobial therapy [18,19], which in many cases could be ineffective due to the lack of information on the causative bacteria. Moreover, aspiration pneumonia is often caused by anaerobes which are hard to culture, further complicating the identification of the causative pathogen [16]. Thus, systematic, culture-independent evaluation of pneumonia-associated oral microbes among long-term care patients could potentially provide information for better antibiotics treatment.

Previous studies [20,21] have addressed the effects of NG tube-feeding on oral microflora with older techniques, e.g. bacterial culture, restriction fragment length polymorphism and pyrosequencing. In this work, we hypothesized that long-term placement of NG tubes alters the composition of the oral microbiome, in a consistent and deterministic manner. First, we sampled from patients' tongues, as indicated by a previous study [22] that the tongue dorsum is the dominant source of microbes to cause aspiration pneumonia. Next, we used Illumina next-generation sequencing (NGS) targeting 16S rRNA amplicons to thoroughly detect the composition of tongue microbiome among NG-tube and oral-feeding patients. In order to achieve high resolution and accuracy in both taxonomic and diversity analysis, we computed amplicon sequence variants (ASV) for both V3 and V4 regions of the 16S rRNA. In this work, we aimed to provide a global picture of the oral microbiomes among NG-tube and oral-feeding patients, which may better inform clinical care practices.

Materials and methods

Patient recruitment and study design

This study involved 53 participants receiving long-term care from the Yilan County, Taiwan, and National Yang Ming Chao Tung University (NYCU) Hospital. Patients were included by the following criteria: (i) receiving long-term care due to moderate-to-severe disability, (ii) stable physical condition and (iii) scheduled for routine dental care. Patients undergoing major medical intervention or antibiotics treatment were excluded. For patients who had been prescribed antibiotics, the last prescription was given at least more than a month before sampling. The recruitment period was from March to October 2021. A total of 26 and 27 patients were nutritionally fed with oral feeding and NG tubes, respectively. Most patients fed with NG-tube resided in the community, receiving home-care dental service.

The study design and patient recruitment procedure was approved by the Ethics Committee of National Yang Ming Chiao Tung University (ID 2020B002). At the beginning of each patient's recruitment, the procedure of the experiments was clearly explained to the participants and their family members, upon which informed consent was obtained. Questionnaires on basic clinical and demographic information on age, sex, systemic diseases, NG tube fixation period and history of pneumonia were filled by either the participants or their family members. A full-mouth oral examination was then performed by the dentist, followed by the collection of tongue plaque samples with sterilized cotton swabs. Regarding gingival status, severe gingivitis was defined by the presence of thick, visible calculus with bleeding gingiva, while mild gingivitis was assigned where there was only bleeding on probing. After sample collection, dental care treatment was performed as the final step of the visit.

Sample preparation and 16S rRNA amplicon sequencing

Tongue samples were collected using sterilized cotton swabs and stored in a fresh, sterile TE buffer (10 mM Tris-HCl pH 8.0, 100 mM EDTA) at 4°C before being transported to the laboratory at AllBio Science Inc., Taichung, Taiwan, for genomic DNA extraction within 24 hours. Total genome DNA was extracted from samples according to the manufacturer's protocol (AllPure Bacteria Genomic DNA Kit). The quality of DNA concentration was controlled by Equalbit dsDNA HS Assay Kit. Samples were then stored at -20°C for preservation before further target PCR amplification and sequencing steps. To avoid confounding batch effects, each batch consisted of two to four randomly assigned samples collected from both NG-tube and oral-feeding patients.

A segment covering hypervariable V3 to V4 regions of the prokaryotic 16S rRNA was used to generate amplicons, by using forward and reverse primers 341F (CCTACGGGNGGCWGCAG) and 805R (GACTACHVGGGTATCTAATCC), respectively [23]. In the second-stage PCR, adapters (P5 and P7) and index sequences were added to either ends of amplified fragments. The DNA library was then purified with magnetic beads (AMPure XP), with concentration and fragment size measured by Qubit™ 3 Fluorometer (Thermo Fisher Scientific) and agarose gel electrophoresis, respectively. The library was adjusted to 10 nM before being sequenced with 150-bp paired-end sequencing on the Illumina MiSeq platform. $78,867 \pm 38,367$ and $77,290 \pm 39,006$ (avg \pm SD) reads ($p = 0.885$, two-tailed unpaired t -test with equal variance) were

sequenced for 27 NG-tube and 26 oral-feeding patients, respectively.

Multivariate logistic regression

Logistic regression was performed using the Python package statsmodels [24]. The dependent (i.e. output) variable was binary NG-tube status. Binary independent variables (pneumonia history, DM status, dementia) were converted to either 0 (absence) or 1 (presence). For gingival status, healthy, mild gingivitis and severe gingivitis were mapped to values 0, 0.5 and 1, respectively, as the three represent increasing severities of gingival illness.

Trimming and demultiplexing

The core of our computational pipeline was built on Qiime2 [25] version 2021.11 (<https://docs.qiime2.org/2021.11/citation/>), with custom numerical analysis implemented with Python (Supplemental Figure S1). To begin, paired-end reads were trimmed with cutadapt [26] wrapped by TrimGalore (<https://github.com/FelixKrueger/TrimGalore>) to remove primer sequences, low-quality bases (minimum Phred quality 20) and reads that were too short (minimum read length 20 bp). Trimmed reads from multiple samples were then imported and demultiplexed as a compressed .qza file to enter the Qiime2 computational ecosystem.

Denoising and taxonomic identification

Using Qiime2, DADA2 denoise algorithm [27] was used to detect ASVs, yielding a feature table (ASV \times sample) and representative sequences for each ASV. Each representative sequence was taxonomically identified by using a pre-trained naive Bayes classifier (<https://data.qiime2.org/2021.8/common/silva-138-99-nb-classifier.qza>) trained on the SILVA database [28]. As each ASV was labeled with its predicted taxon, ASVs of the same taxon were pooled by summing their counts. The 'taxonomic feature pooling' was performed at all taxonomic levels: phylum, class, order, family, genus and species, yielding different levels of taxon tables (taxon \times sample). Taken together, three data entities: (i) feature table (ASV \times sample), (ii) taxon table (taxon \times sample) and (iii) representative sequences were generated at this step for downstream analyses.

Phylogenetic tree

Representative sequences for each ASV were compared using Mafft [29] multiple sequence alignment, generating a FASTA alignment file, from which

FastTree [30] was used to construct both rooted and unrooted phylogenetic trees in Newick (.nwk) format. The whole alignment/tree-building process was executed using the 'qiime phylogeny align-to-tree-mafft-fasttree' command. The Python package ETE Toolkit [31] was used to visualize the phylogenetic tree.

Taxonomic composition

ASV feature counts were combined at all levels of taxonomy (phylum, class, order, family, genus and species) by using Python packages 'numpy' [32], 'pandas' and 'matplotlib'. For each sample, we chose to show the quantity of the 20 most abundant taxa for visual clarity. All the remaining less-abundant taxa were pooled in the 'Others' group.

Log transformation with pseudocount

Count-based analysis methods for high-throughput sequencing are often confounded by numerical overdispersion problems [33]. Similarly, we observed overdispersed ASV counts, spanning 6 orders of magnitude (Supplemental Figure S2a), in which a few dominant ASVs overshadowed other less abundant, yet potentially important ASVs. To alleviate this count overdispersion problem, we applied a log transformation with pseudocount [34] on ASV features, resulting in more evenly distributed abundance values that spanned only 2 orders of magnitude (Supplemental Figure S2b). The 'fat tail' distribution by log-pseudocount made ASVs of all abundance levels more comparable, thus avoiding overdominance by a few extremely abundant ASVs.

Hierarchical clustering

Clustering was performed on all levels of taxonomy (phylum, class, order, family, genus and species). Prior to hierarchical clustering, the ASV feature or taxon counts underwent pseudocount (+1 for each count value) and then log10 transformation. Hierarchical clustering was performed by using the 'clustermap' function of the 'seaborn' package, with default parameters, i.e. 'average' linkage method and 'euclidean' distance metric.

Alpha and beta diversities

From the feature table (ASV \times sample), alpha diversities (observed features and Shannon index) were computed using Qiime2. Wilcoxon rank-sum (i.e. Mann-Whitney U) test was performed with the 'scipy' package. For beta diversity (Bray-Curtis and UniFrac), in addition to Qiime2, Python packages including numpy [32], sklearn [35] and seaborn [36] were also used. Principal coordinate analysis (PCoA) was performed

using the Python package ‘scikit-bio’ and subsequently plotted with ‘seaborn’. Analysis of similarity (ANOSIM) [37] and Mantel test were performed using ‘scikit-bio’.

Differential abundance

LEfSe [38] version 1.1.01 was used. In brief, ‘lefse_run.py’, ‘lefse_plot_res.py’ and ‘lefse_plot_cladogram.py’ were executed in sequence to generate cladograms and LDA plots. Like taxonomic composition analysis and hierarchical clustering, LEfSe was also performed on all taxonomic levels (phylum, class, order, family, genus and species). We presented the LEfSe result on genus and species levels, as they provided the finest taxonomic resolution for differential abundance analysis. Wilcoxon rank-sum (i.e. Mann–Whitney U) test was performed with the ‘scipy’ package.

Spearman’s correlation

The Python package ‘scipy’ was used to compute the correlation coefficient matrix and the corresponding p value matrix. P values were corrected with the Holm–Bonferroni method [39] by using the Python package ‘statsmodels’. Using an adjusted p value ≤ 0.05 as the threshold, only significant correlation coefficient values were shown.

Software integration and interface

The complete data-analysis pipeline (Supplemental Figure S1) was fully integrated with Python, with which we provided a simple, executable command-line interface (CLI). The source code is available at https://github.com/linyc74/qiime2_pipeline and containerized at <https://hub.docker.com/repository/docker/linyc74/qiime2-pipeline>. The complete data

repository is available at <https://dataverse.lib.nyu.edu.tw/dataset.xhtml?persistentId=doi:10.57770/ZJP4B5>.

Results

Patient characteristics and oral health status

A total of 53 patients were recruited between March and October 2021 (Figure 1). Table 1 summarizes all participants’ clinico-demographic background and oral health status. Notably, history of pneumonia was more frequently observed in the NG-tube (63%) than the oral-feeding (12%) group. In addition, patients fed with NG tubes presented higher caries index, residual root calculus and more severe gingivitis. Multivariate logistic regression was performed to reveal the association of NG tube with other systemic and oral factors, among which pneumonia showed the highest coefficient (Supplemental Table S1). Overall, NG-tube patients presented worse general and oral health conditions compared to those fed orally.

V3 and V4 regions yielded consistent taxonomic composition and alpha diversity

The choice of marker gene sequence (i.e. variable regions of 16S rRNA) is critical in accurately resolving microbial diversity and composition. To increase the sequence diversity of the marker gene, we used 341F and 805R to amplify a 465 bp fragment that covers both V3 and V4 regions of 16s rRNA. A total of 150 bp was sequenced with Illumina paired-end sequencing, with read 1 and read 2 covering V3 and V4 regions, respectively. As read 1 and read 2 do not overlap, paired-end reads cannot be merged as a single marker sequence, and should be treated as two separate markers. Thus, we ran the computational pipeline separately on read 1 (V3 region) and read 2 (V4 region) sequences with

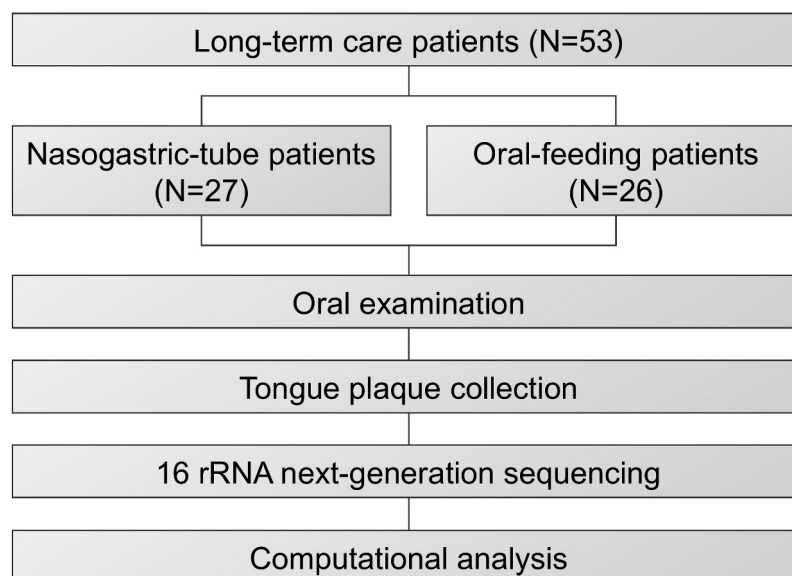


Figure 1. Flow chart of study design.

Table 1. Patient characteristics and oral health status.

		NG-tube patients (N = 27)		Oral-feeding patients (N = 26)	
Age and Sex	Male/Female	8/19		14/12	
	Mean age (SD)	73.92 (22.74)		65.76 (16.77)	
Disability level	Moderate	1	4%	7	27%
	Severe	13	48%	14	54%
	Profound	13	48%	5	19%
Diseases	Hypertension	15	56%	12	46%
	Diabetes mellitus	5	19%	10	38%
	Cardiovascular disease	15	56%	8	31%
	Dementia	8	30%	5	19%
	Liver disease	5	19%	1	4%
	Kidney disease	5	19%	7	27%
Pneumonia history	Yes	16	59%	3	12%
	No	11	41%	23	88%
Bedridden	Yes	26	96%	8	31%
	No	1	4%	18	69%
Dental caries	Decay	5	19%	7	27%
	Missing	5	19%	6	23%
Residual root	Yes	12	44%	11	42%
	No	15	56%	15	58%
Gingival status	Healthy	0	0%	4	15%
	Mild	4	15%	8	31%
	Severe	23	85%	14	54%
Dental Prosthetics	Partial	0	0%	2	8%
	Full mouth	0	0%	3	12%
	Crown/Bridge	9	33%	9	35%

identical configurations. Our result was consistent with a previous study on 16S sequence variability [40], which read 2 (V4 region) identified fewer species than read 1 (V3 region) (Figure 2a). Nonetheless, the percentages unique to and shared by both feeding methods were consistent across read 1 and read 2 (Figure 2a). Detailed genus compositions of each sample were nearly identical between read 1 and read 2 (Supplemental Figure S3). Consequently, alpha diversity indexes (observed features and Shannon entropy) were consistent across read 1 and read 2, and showed no difference between NG-tube and oral-feeding groups (Figure 2b–d). Together, our computational analysis performed robustly and consistently across the V3 and V4 regions of 16S rRNA.

Given the consistency between read 1 and read 2's analyses, we pooled paired-end reads for subsequent computational analysis, to achieve maximum sequence diversity and taxonomic resolution. The Venn diagram based on pooled paired-end reads (Figure 2a, right panel) showed the same percentages as those of read 1 (Figure 2a, left panel), indicating the validity of the pooling approach. Pooling the two target sequences would approximately double the amount of ASVs, achieving a total of 5,480 ASV features from 53 patient samples. The phylogenetic tree of all detected ASVs showed major phylum clades including Firmicutes, Bacteroidota, Actinobacteriota and Proteobacteria (Supplemental Figure S4).

Unsupervised hierarchical clustering showed distinct patterns of microbial composition between NG-tube and oral-feeding groups

Using pooled analysis on V3 and V4 sequences, we set off to examine detailed taxonomic compositions of tongue

microbiome from NG-tube and oral-feeding patients. The 20 most abundant genera shown in Figure 3a were commonly observed in previous studies, including *Streptococcus*, *Neisseria*, *Actinomyces*, *Veillonella*, *Corynebacterium*, *Pseudomonas*, *Fusobacterium* and *Porphyromonas*. We then examined whether NG tube and oral feeding has an effect on microbial composition. We converted the count of each genus to log-pseudocount, and applied unsupervised hierarchical clustering on the genera table (sample × genus). In the heatmap (Figure 3b), distinct patterns were observed between NG-tube and oral-feeding samples, resulting in a nearly complete separation of two clades corresponding to the two feeding methods. We then assigned five groups (I–V) of genera (Figure 3b) based on their overall patterns across all samples, in which group II and IV were enriched in NG-tube and oral-feeding samples, respectively. Generally, more Gram-negatives and a mixture of aerobes, facultatives and anaerobes were found in group II genera (NG tube-associated), whereas group IV (oral feeding-associated) contained mostly Gram-positive anaerobes (Supplemental Table S2). Detailed inspection of the heatmap showed *Corynebacterium* and *Pseudomonas* were among the most overrepresented microbes in NG-tube patients (group II in Figure 3b). Conversely, group IV genera (enriched in oral-feeding patients) include *Veillonella*, *Leptotrichia* and TM7x. Together, distinct compositional patterns of tongue microbiome reflected NG-tube and oral-feeding methods.

Beta diversity showed distinct sample clusters correlated with feeding methods

The distinct patterns of NG-tube and oral-feeding samples in hierarchical clustering (Figure 3b) led us to ask to what extent the tongue microbiomes

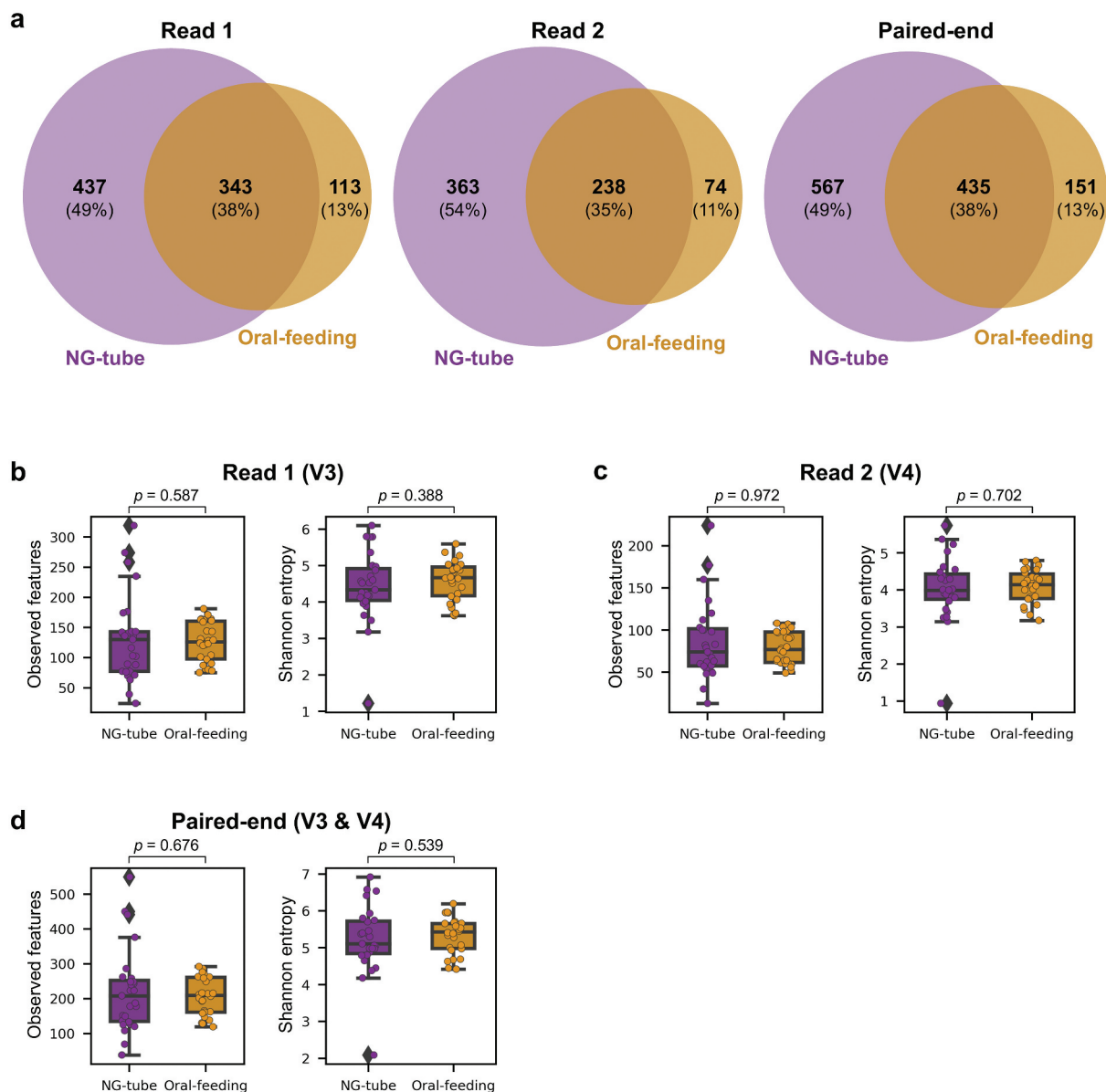


Figure 2. Consistent taxonomic composition and alpha diversity based on read 1 (V3 region) and read 2 (V4 region) sequences. (a) Venn diagrams of species detected from read 1, read 2 and pooled paired-end sequences. (b-d) Alpha diversity (observed features and Shannon entropy) computed from read 1 (b), read 2 (c) and pooled paired-end (d) sequences. P values were determined by Wilcoxon rank-sum test.

differ from each other. We then performed a beta diversity analysis, i.e. sample-to-sample difference, using a total of 5,480 ASV features. Irrespective of the metrics used, the PCoA plots of both Bray-Curtis (Figure 4a) and UniFrac (Supplemental Figure S5) almost completely separated NG-tube and oral-feeding samples, showing significant between-group difference by ANOSIM ($p = 0.00001$). More precisely, the durations of NG-tube placement significantly correlated with beta diversity distances (Mantel test, $p = 0.00003$) (Figure 4b). In addition to feeding methods, we wondered if the segregation pattern could be attributed to other clinical factors. Sample points in the Bray-Curtis PCoA plot (Figure 4a) were colored according to pneumonia history, gingival status,

dementia state and diabetes mellitus (DM) (Figure 4c-f). Among these factors, pneumonia was the only one that resulted in statistical significance ($p = 0.00028$), which could be attributed to the fact that NG-tube patients were correlated with a higher incidence of pneumonia (Table 1 and Supplemental Table S1). In summary, beta-diversity analysis showed that feeding method and history of pneumonia were associated with distinct compositions of tongue microbiomes.

Clinically relevant taxa were associated with NG-tube patients

Given that the tongue samples of NG-tube and oral-feeding patients have significantly different microbial

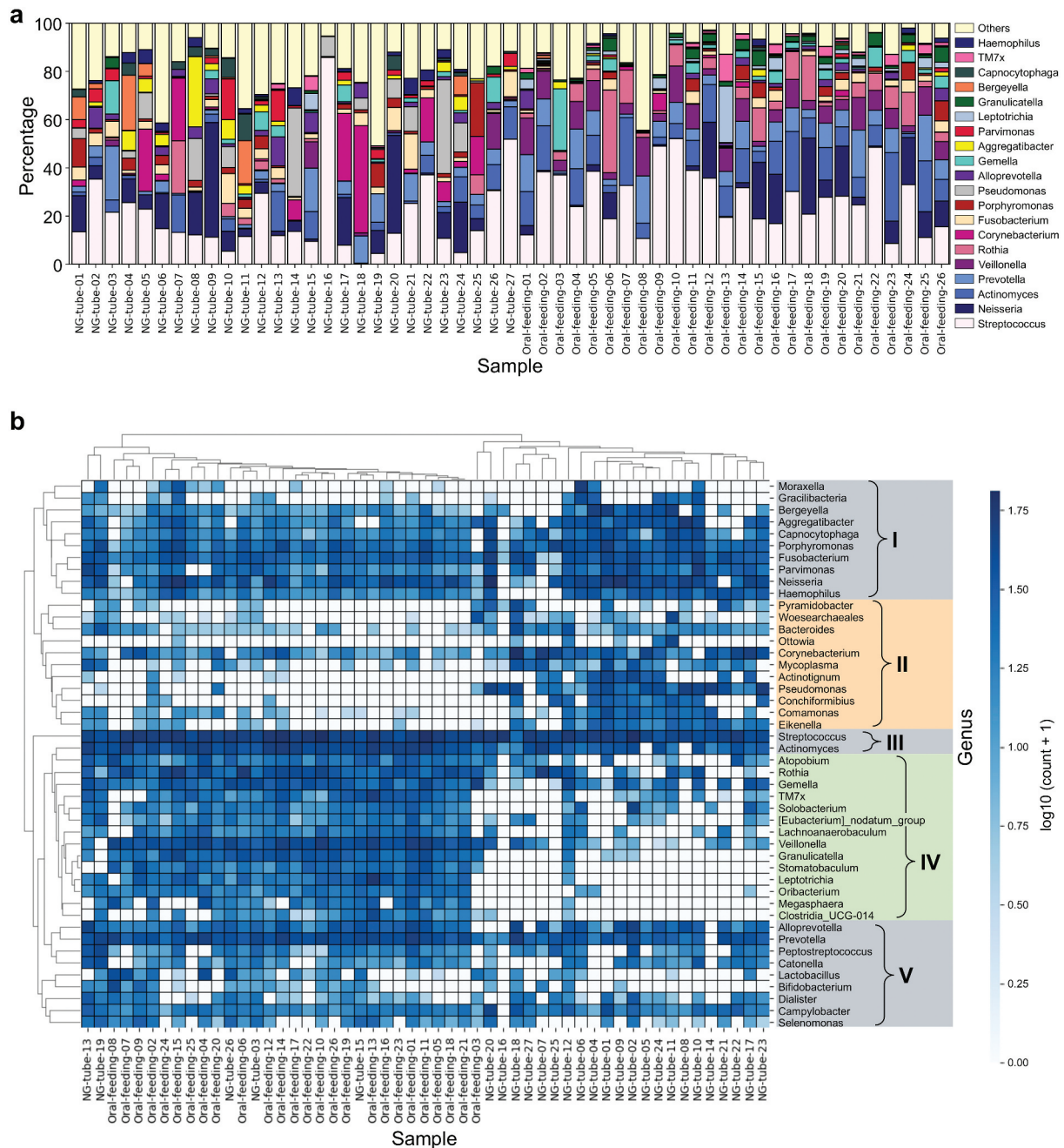


Figure 3. Genus composition and hierarchical clustering of the tongue microbiomes of NG-tube and oral-feeding patients. (a) Bar plot showing the relative abundance of annotated bacterial genera in each sample. Percentages were calculated by raw counts. The 20 most abundant genera across all samples were shown, with the remaining minor genera combined in the group ‘Others’. (b) Heatmap showing unsupervised hierarchical clustering of tongue samples and bacterial genera. Included were the 46 most abundant genera covering 95% of total reads. Five groups of genera were denoted from ‘I’ to ‘V’. Color shades of the heatmap indicate log₁₀ pseudocount values.

composition (Figures 3–4), we sought to identify specific taxa that were overrepresented in either NG-tube or oral-feeding patients. LefSe (Linear Discriminant Analysis Effect Size) was applied on all levels of taxon count tables (phylum, class, order, family, genus, species) to identify NG tube-associated biomarkers. Major clades of phyla were identified in the cladogram (Figure 5a), in which Firmicutes and Actinobacteriota were associated with oral-feeding samples, while Proteobacteria,

Spirochaetota and Synergistota were associated with NG-tube samples.

At the genus level, the two most enriched genera in NG-tube patients were *Corynebacterium* and *Pseudomonas* (Figure 5b), which were validated by Wilcoxon rank-sum test (Figure 6). Specific species of the two genera associated with NG-tube patients include *C. striatum*, *C. casei*, *P. stutzeri*, *P. aeruginosa* and *P. otitidis* (Supplemental Figure S6b). In addition, genus *Parvimonas*, *Fusobacterium*, *Actinotignum* and

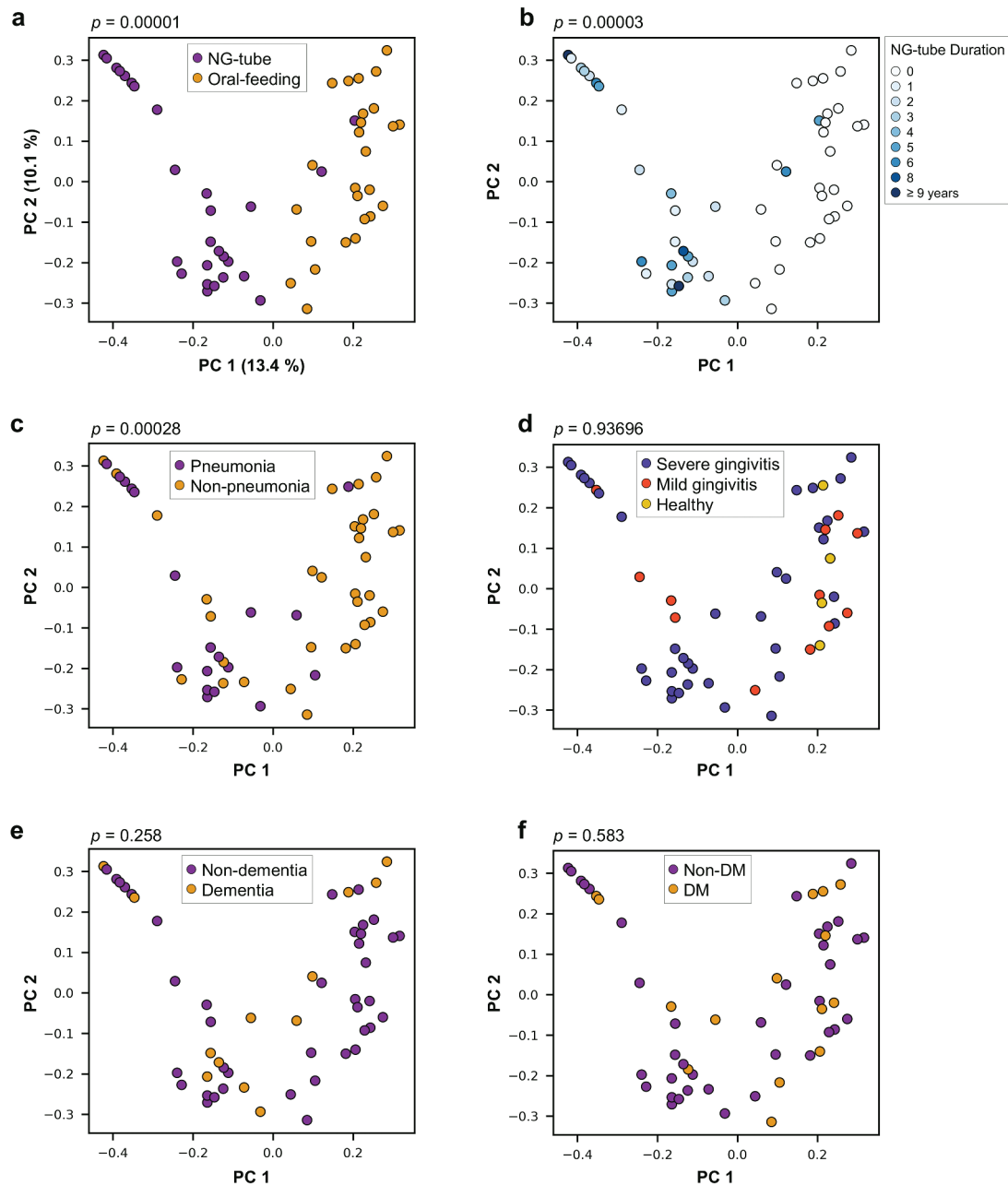


Figure 4. Sample-to-sample difference indicates distinct microbial compositions between NG-tube and oral-feeding samples. Each point in the plot represents a tongue sample, with point-to-point distance indicating Bray-Curtis dissimilarity based on 5,480 ASVs after PCoA dimensionality reduction. Points were colored by feeding method (a), duration of NG tube placement (b), pneumonia history (c), gingival status (d), dementia (e) and DM status (f). Percentages in the parentheses indicate contributions of the two principal components, PC 1 and PC 2. *P* values were determined using ANOSIM (a, c-f) and Mantel test (b) with 99,999 random permutations.

Mycoplasma were associated with NG-tube patients (Figure 5b and Supplemental Figure S7a). As pneumonia history was more prevalent among NG-tube than oral-feeding patients, we also performed LEfSe analysis using pneumonia as the independent factor. Taxa enriched in patients with pneumonia were similar to those associated with NG tubes, including genus *Corynebacterium*, *Pseudomonas*, *Actinotignum* and *Mycoplasma* (Supplemental Figure S8). In oral-feeding patients, *Streptococcus* and *Veillonella* were the most significantly enriched (Figures 5b and 6). Additionally, genus *Actinomyces*, *Rothia*, *Prevotella*, *Leptotrichia*,

Granulicatella and TM7 \times were associated with oral-feeding patients (Figure 5b and Supplemental Figure S7b).

Co-occurrence analysis revealed antagonism between pathogenic and commensal species

We further asked whether the taxa associated with NG tube or oral feeding (Figure 5) would co-occur with one another. We particularly focused on species of the four genera: *Corynebacterium*, *Pseudomonas*, *Streptococcus* and *Veillonella*, as they were either enriched or depleted in the presence of NG tubes

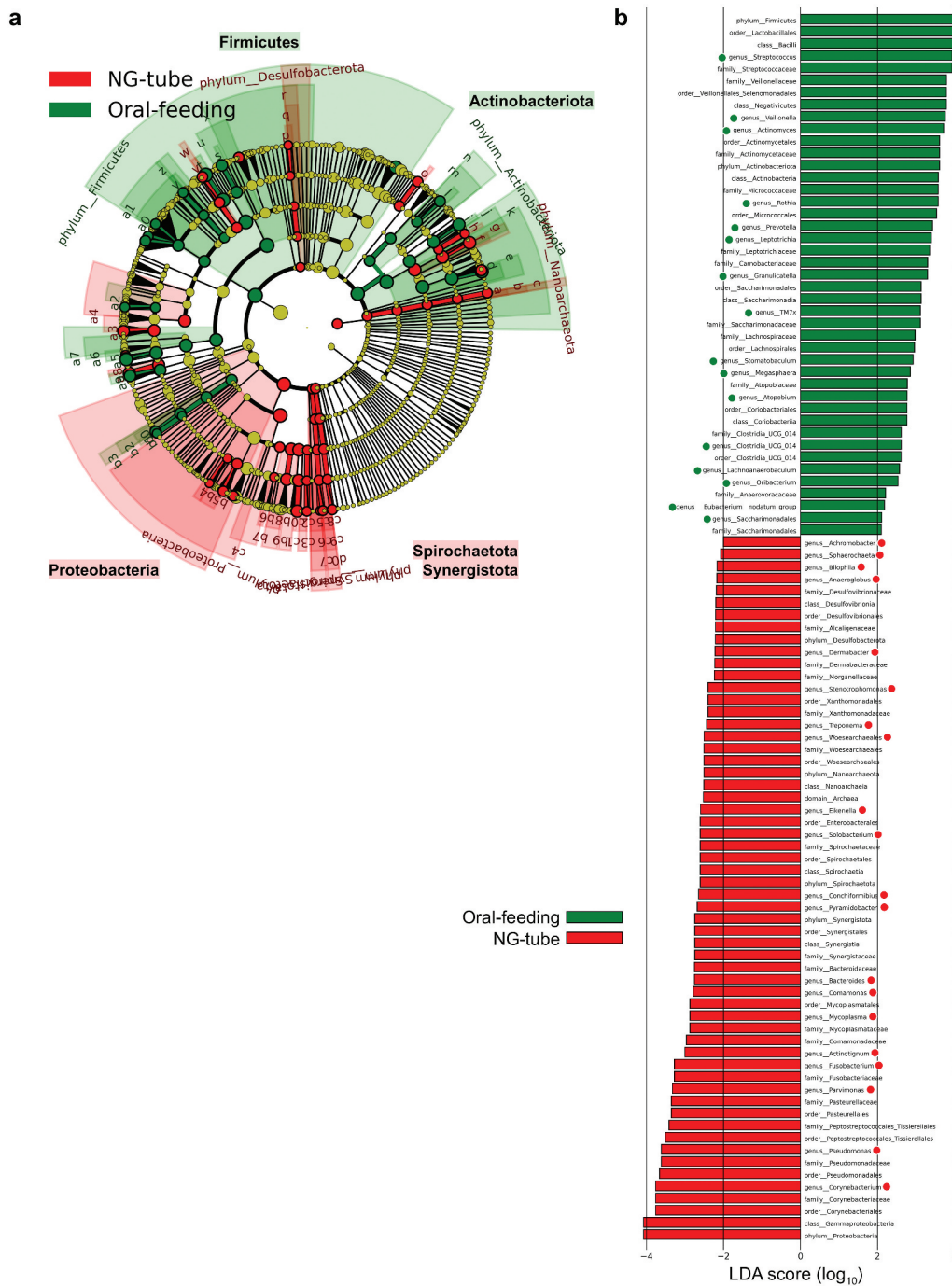


Figure 5. Genus-level LefSe analysis revealed bacterial biomarkers enriched in NG-tube and oral-feeding patients. (a) Cladogram showing major bacterial phylum clades associated with NG-tube and oral-feeding patients. (b) LDA score (min cutoff 2.0) of bacterial biomarkers associated with NG-tube and oral-feeding patients. Red and green dots mark all genus-level biomarkers. Wilcoxon p values ≤ 0.05 .

(Figure 6). Spearman’s correlation coefficient was computed to measure pairwise co-occurrence of species. For visual clarity, we reordered the species in the correlation matrix such that more correlated ones were juxtaposed (Figure 7). Two groups emerged, corresponding to commensals and pathogens associated with oral feeding and NG tube, respectively. The commensal group (Figure 7; upper left) consisted of *Streptococcus* and *Veillonella* species, including *S. pseudopneumoniae*, *S. mitis*, *V. rogosae*, *S. sanguinis*, *V. atypica*, *S. salivarius*, *S. suis* and

S. uberis, whereas the pathogenic group (Figure 7; bottom right) contained mostly *Corynebacterium* and *Pseudomonas*, including *P. otitidis*, *P. aeruginosa*, *C. striatum*, *C. simulans*, *C. casei* and *P. stutzeri*. Interestingly, *Streptococcus infantis* was correlated with *P. otitidis* instead of the commensal Streptococci. Furthermore, a negative correlation was observed between commensals (*S. sanguinis*, *V. atypica*, *S. salivarius*, *S. suis*, *S. uberis*) versus pathogens (*P. aeruginosa*, *C. striatum*, *C. simulans*) (Figure 7; top right and bottom left). Taken together,

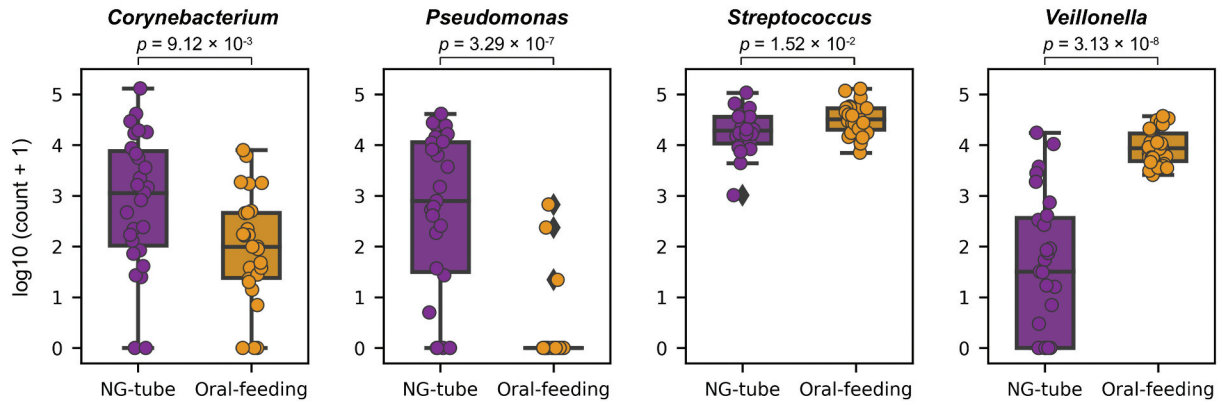


Figure 6. Log₁₀ pseudocounts of four genera enriched in NG-tube (*Corynebacterium* and *Pseudomonas*) and oral-feeding (*Streptococcus* and *Veillonella*) tongue samples. *P* values were determined using Wilcoxon rank-sum test.

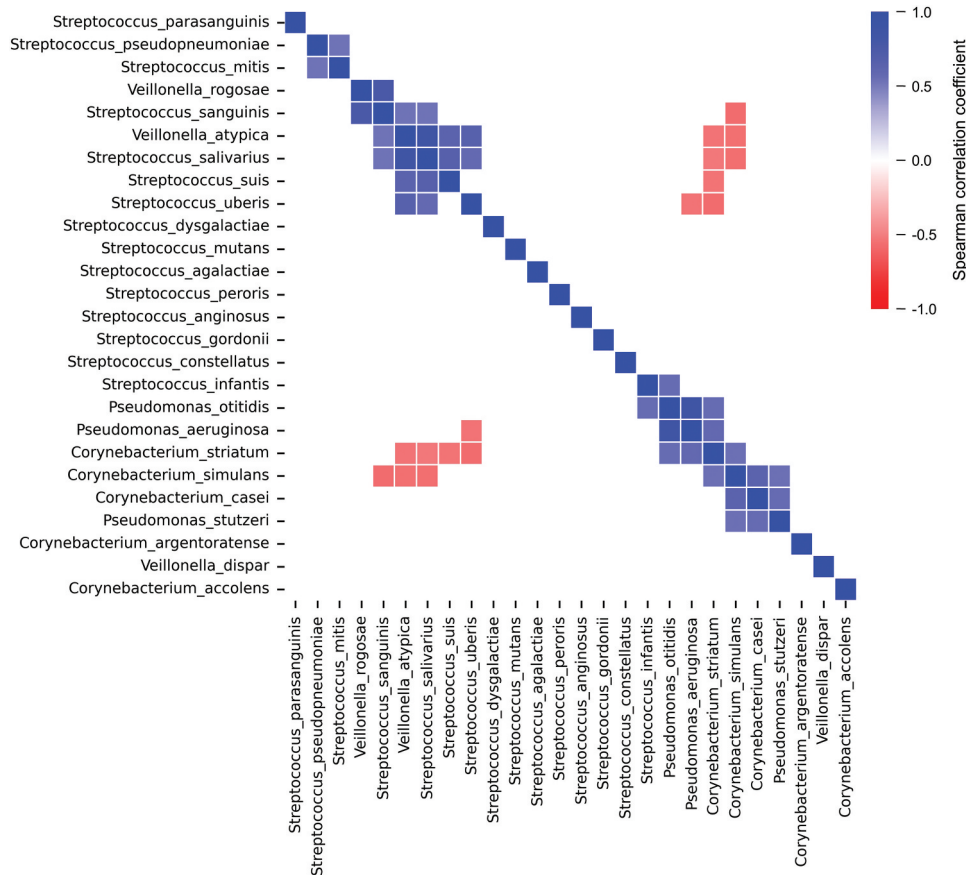


Figure 7. Co-occurrence of species of four genera: *Streptococcus*, *Veillonella*, *Corynebacterium* and *Pseudomonas*, measured by Spearman's correlation. Positive and negative correlation coefficients indicate co-occurrence and mutual exclusion, respectively. Only significant values were shown (Holm-adjusted *p* value ≤ 0.05).

co-occurrence was observed within respective groups of bacteria, whereas an antagonistic relationship existed between the two groups.

Discussion

In this study, we demonstrated that long-term placement of NG tubes significantly altered the composition of the oral microbiome. We found that opportunistic pathogens

like *Pseudomonas* and *Corynebacterium* were associated with NG-tube feeding, and these pathogens were negatively correlated with commensal microbes (e.g. *Streptococcus* and *Veillonella*) that were enriched in oral-feeding patients. Notably, *Corynebacterium* and *Pseudomonas* were both reported to cause aspiration pneumonia [41,42], corroborating the fact that NG-tube patients had a higher incidence of pneumonia (Table 1). Conversely, genera enriched in oral-feeding patients include *Veillonella*, *Streptococcus*, *Leptotrichia* and

TM7×, which were all members of the common oral microflora [1,43]. The co-occurrence of *Streptococcus* and *Veillonella* was not coincidental, as studies [44,45] have demonstrated a symbiotic relationship in which *Veillonella* metabolizes the lactate produced by *Streptococcus*, completing metabolic cross-feeding within a microbial community. Interestingly, interactions between *Streptococcus* and *Veillonella* have been mostly reported in dental plaque [46], whereas our study focused on the tongue dorsum.

A conceptually similar study to ours was conducted by Leibovitz *et al.* [20], in which oral microbes of older, frail patients were examined by using traditional culture-based techniques to detect pathogens. Although definitive, culture-based methods are inherently slow, low-throughput and limited to culturable species. Our work presents a systematic, culture-free and high-resolution profiling of oral microbiome regarding the effect of indwelling NG tubes. Such a study could possibly inform the choice of antimicrobials before specific bacterial culture becomes available. Indeed, high-throughput sequencing has been used for fast, culture-free pathogen identification in various clinical scenarios [47–49].

A general notion exists that long-term fixation of NG tubes impairs swallowing function, thereby increasing the risk of aspiration pneumonia. Studies have shown that community-based older patients fed with NG tubes are generally at high risk of aspiration pneumonia [50]. Moreover, pathogens of community-acquired pneumonia are generally different from those causing hospital-acquired pneumonia and thus require a different set of antimicrobials to treat [15,51]. Our survey of tongue microbes in patients with NG tubes showed mostly Gram-negative bacteria with a mixture of aerobes and anaerobes such as *Pseudomonas*, and also the Gram-positive *Corynebacterium* (Supplemental Table S2). The spectrum of tongue microbes in NG-tube patients may provide predictive information for empiric antimicrobial therapy.

This observational study was not aimed at establishing any causal relationship between the placement of NG tubes and changes in the oral microbiome. Patients with NG tubes were inherently more ill with impaired oral functions, which may influence the oral microbiome via a multitude of mechanisms. The findings of this study are the results of complex host factors associated with the physiologic condition under NG tube-feeding. Nonetheless, identifying NG tube-associated oral pathogens would still be of value for antimicrobial therapy, or other clinical assessments concerning oral bacteria.

Challenges remain for microbiome study, one of them being the technical limitation to a small number of hypervariable regions of 16S rRNA. To solve this problem, complete sequences of 16S rRNA need to be unambiguously defined, for which long-read

sequencing technology such as PacBio SMRT has been applied [40]. Nonetheless, even with the complete sequence of 16S rRNA, target genes are at best ‘proxy’ for species identification, but not the comprehensive picture of physiologic and pathogenic functions. Virulence is essentially driven by microbial functions, not taxonomy. Supporting this notion, metabolic functions were shown to be well conserved across microbiomes from various body sites, despite radically different taxonomic compositions [43]. With constant advancement in sequencing throughput, shotgun metagenomic studies have emerged to functionally elucidate oral microbiome [52]. In the future, the use of long-read sequencing combined with shotgun functional metagenomics will shed new light on the complexity of the human oral microbiome.

Finally, our study in Taiwan presented strikingly similar findings to the study by Takeshita *et al.* [21] a decade ago in Japan, in which NG-tube patients harbored more opportunistic pathogens like *Corynebacterium* and less commensal *Streptococcus* and *Veillonella*. Cross-national evidence indicates that long-term NG-tube feeding has predictable and deterministic effects on the oral microbiome, and thus indications for an antimicrobial regimen.

Acknowledgments

The authors sincerely thank the support from the Department of Dentistry, National Yang Ming Chao Tung University Hospital, and all the participants in this study. This work was supported by the Ministry of Science and Technology, Taiwan under grant IDs ‘111-2314-B-A49-087-MY3’, ‘110-2314-B-A49A-519’, ‘111-2314-B-A49-028-MY2’, ‘109-2314-B-010-012-MY2’ and ‘110-2314-B-A49A-551’, as well as the Yen Tjing Ling Medical Foundation under the grant ID ‘CI-111-18’. The authors report there are no conflicts of interest to disclose.




Disclosure statement

No potential conflict of interest was reported by the authors.

Funding

The work was supported by the Ministry of Science and Technology, Taiwan [111-2314-B-A49-087-MY3]; Ministry of Science and Technology, Taiwan [109-2314-B-010-012-MY2]; Ministry of Science and Technology, Taiwan [110-2314-B-A49A-519]; Ministry of Science and Technology, Taiwan [110-2314-B-A49A-551]; Ministry of Science and Technology, Taiwan [111-2314-B-A49-028-MY2]; Yen Tjing Ling Medical Foundation [CI-111-18]

ORCID

Ding-Han Wang  <http://orcid.org/0000-0003-3314-6113>
 Fa-Tzu Tsai  <http://orcid.org/0000-0002-0468-2614>
 Hsi-Feng Tu  <http://orcid.org/0000-0003-0177-6065>

Cheng-Chieh Yang  <http://orcid.org/0000-0002-5355-0087>

Ming-Lun Hsu  <http://orcid.org/0000-0001-6753-0485>

Yu-Cheng Lin  <http://orcid.org/0000-0002-4787-2565>

References

- [1] Dewhirst FE, Chen T, Izard J, et al. The human oral microbiome. *J Bacteriol.* 2010;192:5002–5017.
- [2] Willis JR, Gabaldón T. The human oral microbiome in health and disease: from sequences to ecosystems. *Microorganisms.* 2020;8:308.
- [3] Peng X, Cheng L, You Y, et al. Oral microbiota in human systematic diseases. *Int J Oral Sci.* 2022;14:14.
- [4] Del Giudice C, Vaia E, Liccardo D, et al. Infective endocarditis: a focus on oral microbiota. *Microorganisms.* 2021;9:1218.
- [5] Healy CM, Moran GP. The microbiome and oral cancer: more questions than answers. *Oral Oncol.* 2019;89:30–33.
- [6] Do T, Dame-Teixeira N, Deng D. Editorial: applications of next generation sequencing (NGS) technologies to decipher the oral microbiome in systemic health and disease. *Front Cell Infect Microbiol.* 2021;11:11.
- [7] Lamont RJ, Koo H, Hajishengallis G. The oral microbiota: dynamic communities and host interactions. *Nat Rev Microbiol.* 2018;16:745–759.
- [8] Ogawa T, Hirose Y, Honda-Ogawa M, et al. Composition of salivary microbiota in elderly subjects. *Sci Rep.* 2018;8:414.
- [9] Jaafar MH, Mahadeva S, Morgan K, et al. Percutaneous endoscopic gastrostomy versus nasogastric feeding in older individuals with non-stroke dysphagia: a systematic review. *J Nutr Health Aging.* 2015;19:190–197.
- [10] Chen X, Clark JJ, Chen H, et al. Cognitive impairment, oral self-care function and dental caries severity in community-dwelling older adults. *Gerodontology.* 2015;32:53–61.
- [11] Chauhan D, Varma S, Dani M, et al. Nasogastric tube feeding in older patients: a review of current practice and challenges faced. *Curr Gerontol Geriatr Res.* 2021;2021:6650675.
- [12] Dziejwas R, Warnecke T, Hamacher C, et al. Do nasogastric tubes worsen dysphagia in patients with acute stroke? *BMC neurol.* 2008;8:28.
- [13] Volkert D, Pauly L, Stehle P, et al. Prevalence of malnutrition in orally and tube-fed elderly nursing home residents in Germany and its relation to health complaints and dietary intake. *Gastroenterol Res Pract.* 2011;2011:247315.
- [14] Kim G, Baek S, Park H-W, et al. Effect of nasogastric tube on aspiration risk: results from 147 patients with dysphagia and literature review. *Dysphagia.* 2018;33:731–738.
- [15] Mandell LA, Niederman MS, Longo DL. Aspiration Pneumonia. *N Engl J Med.* 2019;380:651–663.
- [16] Otsuji K, Fukuda K, Ogawa M, et al. Dynamics of microbiota during mechanical ventilation in aspiration pneumonia. *BMC Pulm Med.* 2019;19:260.
- [17] Gomes GF, Pisani JC, Macedo ED, et al. The nasogastric feeding tube as a risk factor for aspiration and aspiration pneumonia. *Curr Opin Clin Nutr Metab Care.* 2003;6:327–333.
- [18] Leekha S, Terrell CL, Edson RS. General principles of antimicrobial therapy. *Mayo Clin Proc.* 2011;86:156–167.
- [19] TM F Jr, Niederman MS. Antimicrobial therapy of community-acquired pneumonia. *Infect Dis Clin North Am.* 2004;18:993–1016, xi.
- [20] Leibovitz A, Plotnikov G, Habet B, et al. Pathogenic colonization of oral flora in frail elderly patients fed by nasogastric tube or percutaneous enterogastric tube. *J Gerontol A Biol Sci Med Sci.* 2003;58:52–55.
- [21] Takeshita T, Yasui M, Tomioka M, et al. Enteral tube feeding alters the oral indigenous microbiota in elderly adults. *Appl Environ Microbiol.* 2011;77:6739–6745.
- [22] Asakawa M, Takeshita T, Furuta M, et al. Tongue microbiota and oral health status in community-dwelling elderly adults. *mSphere.* 2018;3:3.
- [23] Sinclair L, Osman OA, Bertilsson S, et al. Microbial community composition and diversity via 16S rRNA gene amplicons: evaluating the illumina platform. *PLoS ONE.* 2015;10:e0116955.
- [24] Seabold S, Perktold J Statsmodels: econometric and statistical modeling with python. Proceedings of the 9th Python in Science Conference. *SciPy;* 2010. doi:10.25080/majora-92bf1922-011
- [25] Bolyen E, Rideout JR, Dillon MR, et al. Reproducible, interactive, scalable and extensible microbiome data science using QIIME 2. *Nat Biotechnol.* 2019;37:852–857.
- [26] Martin M. Cutadapt removes adapter sequences from high-throughput sequencing reads. *EMBnet J.* 2011;17:10–12.
- [27] Callahan BJ, McMurdie PJ, Rosen MJ, et al. DADA2: high-resolution sample inference from Illumina amplicon data. *Nat Methods.* 2016;13:581–583.
- [28] Quast C, Pruesse E, Yilmaz P, et al. The SILVA ribosomal RNA gene database project: improved data processing and web-based tools. *Nucleic Acids Res.* 2013;41:D590–6.
- [29] Katoh K, Misawa K, Kuma K-I, et al. MAFFT: a novel method for rapid multiple sequence alignment based on fast Fourier transform. *Nucleic Acids Res.* 2002;30:3059–3066.
- [30] Price MN, Dehal PS, Arkin AP. FastTree 2 – approximately maximum-likelihood trees for large alignments. *PLoS ONE.* 2010;5:e9490.
- [31] Huerta-Cepas J, Serra F, Bork P. ETE 3: reconstruction, analysis, and visualization of phylogenomic data. *Mol Biol Evol.* 2016;33:1635–1638.
- [32] Harris CR, Millman KJ, van der Walt SJ, et al. Array programming with NumPy. *Nature.* 2020;585:357–362.
- [33] Zhang H, Pounds SB, Tang L. Statistical methods for overdispersion in mRNA-seq count data. *Open Bioinforma J.* 2013;7:34–40.
- [34] Ahlmann-Eltze C, Huber W. Transformation and pre-processing of single-cell RNA-Seq data. *bioRxiv.* 2021;2021.06.24.449781. DOI:10.1101/2021.06.24.449781
- [35] Buitinck L, Louppe G, Blondel M, et al. API design for machine learning software: experiences from the scikit-learn project. *arXiv [cs.LG].* 2013. Available: <http://arxiv.org/abs/1309.0238>
- [36] Waskom M. Seaborn: statistical data visualization. *J Open Source Softw.* 2021;6:3021.
- [37] Clarke KR. Non-parametric multivariate analyses of changes in community structure. *Austral Ecol.* 1993;18:117–143.

- [38] Segata N, Izard J, Waldron L, et al. Metagenomic biomarker discovery and explanation. *Genome Biol.* **2011**;12:R60.
- [39] Holm S. A simple sequentially rejective multiple test procedure. *Scand Stat Theory Appl.* **1979**;6:65–70.
- [40] Johnson JS, Spakowicz DJ, Hong B-Y, et al. Evaluation of 16S rRNA gene sequencing for species and strain-level microbiome analysis. *Nat Commun.* **2019**;10:5029.
- [41] Yang K, Kruse RL, Lin WV, et al. *Corynebacteria* as a cause of pulmonary infection: a case series and literature review. *Pneumonia (Nathan).* **2018**;10:10.
- [42] Fujitani S, Sun H-Y, Yu VL, et al. Pneumonia due to *Pseudomonas aeruginosa*: part I: epidemiology, clinical diagnosis, and source. *Chest.* **2011**;139:909–919.
- [43] Human Microbiome Project Consortium. Structure, function and diversity of the healthy human microbiome. *Nature.* **2012**;486:207–214.
- [44] Hughes CV, Kolenbrander PE, Andersen RN, et al. Coaggregation properties of human oral *Veillonella* spp.: relationship to colonization site and oral ecology. *Appl Environ Microbiol.* **1988**;54:1957–1963.
- [45] Mashima I, Nakazawa F, O'Toole GA. The interaction between *Streptococcus* spp. and *Veillonella tobetsuensis* in the early stages of oral biofilm formation. *J Bacteriol.* **2015**;197:2104–2111.
- [46] Chalmers NI, Palmer RJ Jr, Cisar JO, et al. Characterization of a *Streptococcus* sp.-*Veillonella* sp. community micromanipulated from dental plaque. *J Bacteriol.* **2008**;190:8145–8154.
- [47] Gu W, Deng X, Lee M, et al. Rapid pathogen detection by metagenomic next-generation sequencing of infected body fluids. *Nat Med.* **2021**;27:115–124.
- [48] Gwinn M, MacCannell D, Armstrong GL. Next-generation sequencing of infectious pathogens. *JAMA.* **2019**;321:893–894.
- [49] Frey KG, Bishop-Lilly KA. Chapter 15 - next-generation sequencing for pathogen detection and identification. In: Sails A Tang Y-W, editors. *Methods in Microbiology.* Academic Press; **2015.** pp. 525–554.
- [50] Marin-Corral J, Pascual-Guardia S, Amati F, et al. Aspiration risk factors, microbiology, and empiric antibiotics for patients hospitalized with community-acquired Pneumonia. *Chest.* **2021**;159:58–72.
- [51] Lanks CW, Musani AI, Hsia DW. Community-acquired Pneumonia and Hospital-acquired Pneumonia. *Med Clin North Am.* **2019**;103:487–501.
- [52] Utter DR, Borisy GG, Eren AM, et al. Metapangenomics of the oral microbiome provides insights into habitat adaptation and cultivar diversity. *Genome Biol.* **2020**;21:293.